

The Impact of Interference on GNSS Receiver Observables – A Running Digital Sum Based Simple Jammer Detector

Mohammad Zahidul H. BHUIYAN¹, Heidi KUUSNIEMI¹, Stefan SÖDERHOLM¹, Esa AIROS²

¹Dept. of Navigation and Positioning, Finnish Geodetic Institute, Kirkkonummi, Finland

²Defence Forces Technical Research Centre, Riihimäki, Finland

zahidul.bhuiyan@fgi.fi, heidi.kuusniemi@fgi.fi, stefan.soderholm@fgi.fi, esa.airos@mil.fi

Abstract. *A GNSS-based navigation system relies on externally received information via a space-based Radio Frequency (RF) link. This poses susceptibility to RF Interference (RFI) and may initiate failure states ranging from degraded navigation accuracy to a complete signal loss condition. To guarantee the integrity of the received GNSS signal, the receiver should either be able to function in the presence of RFI without generating misleading information (i.e., offering a navigation solution within an accuracy limit), or the receiver must detect RFI so that some other means could be used as a countermeasure in order to ensure robust and accurate navigation. Therefore, it is of utmost importance to identify an interference occurrence and not to confuse it with other signal conditions, for example, indoor or deep urban canyon, both of which have somewhat similar impact on the navigation performance. Hence, in this paper, the objective is to investigate the effect of interference on different GNSS receiver observables in two different environments: i. an interference scenario with an inexpensive car jammer, and ii. an outdoor-indoor scenario without any intentional interference. The investigated observables include the Automatic Gain Control (AGC) measurements, the digitized IF (Intermediate Frequency) signal levels, the Delay Locked Loop and the Phase Locked Loop discriminator variances, and the Carrier-to-noise density ratio (C/N_0) measurements. The behavioral pattern of these receiver observables is perceived in these two different scenarios in order to comprehend which of those observables would be able to separate an interference situation from an indoor scenario, since in both the cases, the resulting positioning accuracy and/or availability are affected somewhat similarly. A new Running Digital Sum (RDS) -based interference detection method is also proposed herein that can be used as an alternate to AGC-based interference detection. It is shown in this paper that it is not at all wise to consider certain receiver observables for interference detection (i.e., C/N_0); rather it is beneficial to utilize certain specific observables, such as the RDS of raw digitized signal levels or the AGC-based observables that can uniquely identify a critical malicious interference occurrence.*

Keywords

GNSS, jamming, in-car jammer, interference detection, receiver observables.

1. Introduction

Global Navigation Satellite System (GNSS) based positioning has an immense role in modern society. Reliable navigation is imperative in more and more applications nowadays on land, sea, and air. A major dependency on reliable localization has been emerging, especially within safety-critical applications [1]. GNSS signals, as well as many other Radio Frequency (RF) signals, are however extremely susceptible to unintentional and intentional malicious interference. Since GNSS signals are also very weak, after travelling the distance of about 20000 km from the satellite to the Earth, they can be very difficult to recover when subject to interference.

Applications using GNSS based positioning for road tolling, insurance billing, or logistics have increased recently in quantity. Simultaneously, despite being illegal, intentional jamming of the related satellite navigation receivers has become temptingly easy. Though illegal, affordable jammer devices can easily be purchased online or built according to widely attainable online recipes. The increase in the amount of satellite navigation jammers is alarming, especially due to the serious damage they may cause. Because satellite positioning is in such a vital role in many applications, jammers may cause great damage if not detected and their effects mitigated. The typical usage environment of jammers is in cars, where they transmit a jamming signal usually on the civilian L1/E1-band where the accessible GPS C/A and the upcoming civilian Galileo codes are located. Civilian in-car jammers pose a severe threat to the trustworthiness of GNSS receivers [2]-[4]. High-power jammers may not only hinder the usage of GNSS in the vicinity of the jammer but also paralyze GNSS usage over a larger area.

The jamming signal may deteriorate the position solution or totally induce loss of lock of GNSS signals depending on the perceived Jamming-to-Signal (J/S) power ratio at the receiver [5], [6]. Different receivers react differently to jamming depending on the properties of the jamming signal. The basic functionalities in most GNSS receivers are fairly similar, but the internal architecture and algorithms vary. Different kinds of filtering may for example mitigate the effect of the jammer on the positioning accuracy and availability. Intentional GNSS jamming raises the noise floor and thus reduces the Carrier-to-Noise density ratio (C/N_0) of the received signals. This effect is similar to the phenomenon perceived in the context of multipath propagation or general signal attenuation due to for example foliage: in such a case the received signals become weaker, also resulting in lower C/N_0 measurements. When the C/N_0 is low enough, the receiver cannot anymore generate ranging measurements and the position solution cannot be computed.

In order to mitigate the effects of interference from intentional or unintentional sources, reliable interference detection must be conducted first. In [7] and [8], interference detection is performed based on a combination of several receiver observables, i.e., correlator output power, variance of correlator output power, carrier phase vacillation, and AGC (Automatic Gain Control) values. The studies reported in [8] are mainly based on simulated signals for different kinds of interference, for example, AWGN, Continuous Wave (CW), pulsed broadband, pulsed CW, etc. It is concluded in [8] that the correlator output power showed the best consistent performance under varying level as well as varying sources of interference. The impact of various types of interference on AGC circuit is also studied in [9], [10], and it is concluded that the AGC can be used as an interference assessment tool for GNSS receivers.

The objective of this research is to investigate the effect of inexpensive in-car jammers on different GNSS receiver observables. The investigated observables include the Automatic Gain Control (AGC) measurements, the digitized IF (Intermediate Frequency) signal levels, the Delay Locked Loop, the Phase Locked Loop discriminator variances, and the Carrier-to-noise density ratio (C/N_0) measurements. The reason for choosing these observables is motivated by the fact that all observables except AGC are instantly available at the signal processing stage, and can be utilized solely in a software-defined GNSS receiver. The software-defined receivers are useful tools for research purposes and are beneficial for testing and implementing various algorithms before hardware implementation. However, it is little bit tricky to obtain access to AGC observables, as the front-end manufacturers do not usually offer access to an AGC circuit. In this study, the AGC voltage test pin was used to measure the level of the gain control in the various scenarios. The selection of the observables assessed in this paper for interference detection is also in line with other previous studies on the topic mentioned in

[7]-[9]. The behavioral pattern of these receiver observables is perceived in the presence of interference and in indoor signal condition without any intentional jamming. The authors also introduce a unique Running Digital Sum (RDS) based interference detection method for GNSS signals. In this method, the interference detection is performed via a Running Digital Sum (RDS) [11], [12] check of the digitized signal after the Analog-to-Digital Conversion (ADC) at the intermediate frequency. As shown later, the introduced RDS based interference detection method can successfully distinguish the intentional interference occurrence from that of a weak indoor signal condition.

The remaining of this paper is organized as follows. Section 2 briefly characterizes the cheap car-jammer used in the experiment. In Section 3, all the considered receiver observables used for jamming detection are discussed. Experimental setup and result analysis are presented in Sections 4 and 5, respectively. Finally, some concluding remarks are made in Section 6 based on the experimental results.

2. Jammer Characterization

The increase in the amount of satellite navigation jammers is alarming due to the serious harm they may cause. The typical usage environment of jammers is in cars, where they act as so called personal privacy devices and transmit a jamming signal usually on the civilian L1/E1-band. A car jammer, the Covert GPS L1 jammer is used in the experiment. The Covert L1 jammer is shown in Fig. 1.

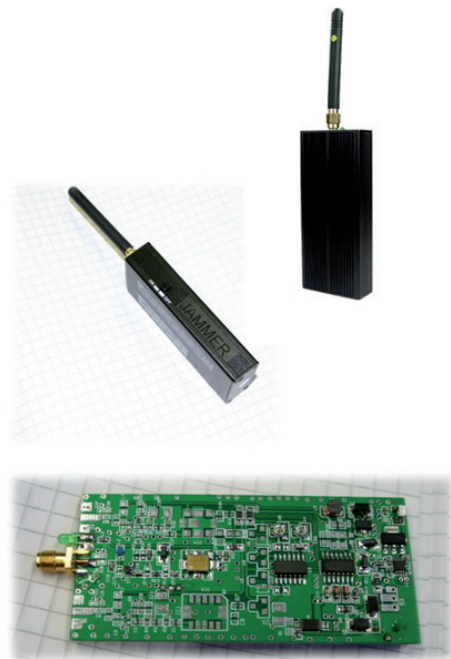


Fig. 1. Covert GPS L1 jammer.

A constrained usage permission of the jammer was obtained from the Finnish Communications Regulatory

Authorities. According to the permission, the jammer has to be used within the laboratory of the Finnish Geodetic Institute (FGI) only for the purpose of research. The output power of the jammer was measured to be around +18 dBm, and it transmits chirp-like signals. A chirp signal (also known as sweep signal) is a signal in which the frequency increases ('up-chirp') or decreases ('down-chirp') with time. The Covert L1 jammer transmits a chirp signal with multi saw-tooth functions having a center frequency at approximately 1.577 GHz with a bandwidth of about 16.3 MHz. The power spectrum and the instantaneous frequency of the jammer are shown in Figs. 2 and 3, respectively. The characteristics of Covert L1 jammer coincide very well with the findings reported in [2], [3].

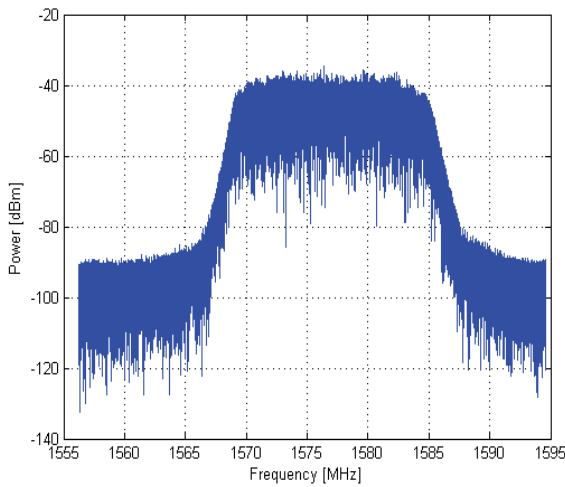


Fig. 2. Power spectrum of the Covert GPS L1 jammer.

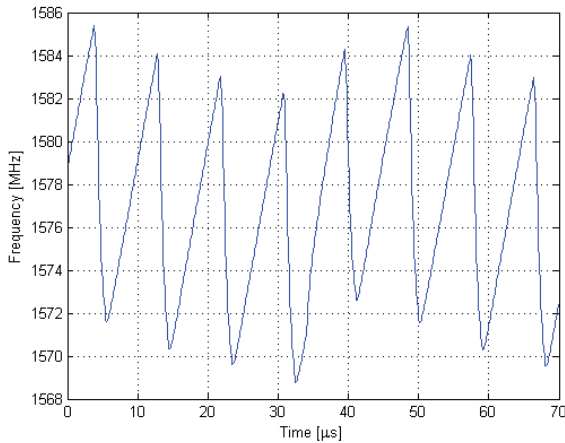


Fig. 3. Instantaneous frequency of the Covert GPS L1 jammer.

3. Observables Used for Jammer Detection

The following receiver observables are considered throughout the experiment for jamming detection:

- i) Carrier-to-Noise density ratio,

- ii) Running DLL variance,
- iii) Running PLL variance,
- iv) Automatic Gain Control level changing rate, and
- v) Running digital sum of the IF data samples.

As mentioned earlier, the reason for choosing these observables is motivated by the fact that all observables except AGC are instantly available at the signal processing stage, and can be utilized solely in a software-defined GNSS receiver. A brief overview on each of these receiver observables is presented in what follows.

3.1 Carrier-to-Noise Density Ratio

Carrier-to-Noise density ratio (C/N_0) is used to measure the strength of a received GNSS signal. The Carrier-to-Noise density ratio (C/N_0) estimation is performed based on the ratio of the signal's wideband power to its narrow-band power as mentioned in [5]:

$$C/N_0 = 10 \log_{10} \left(\frac{1}{T} \frac{\hat{\mu}_{NP} - 1}{M - \hat{\mu}_{NP}} \right) \quad (1)$$

where T is the code integration time in seconds (i.e., 0.001 s for GPS L1 C/A signal); M is the total number of T blocks used for coherent integration (usually a fair choice of $M = 20$ is used as the data bit duration for GPS L1 C/A signal is 20 ms), and $\hat{\mu}_{NP}$ is the mean normalized power, as expressed in the following equation:

$$\hat{\mu}_{NP} = \frac{1}{K} \sum_{k=1}^K NP_k \quad (2)$$

where NP is the normalized power between narrow-band power and wide-band power:

$$NP_k = \frac{NBP_k}{WBP_k} \quad (3)$$

where NBP and WBP can be expressed as follows:

$$NBP_k = \left(\sum_{i=1}^M I_{P_i} \right)_k^2 + \left(\sum_{i=1}^M Q_{P_i} \right)_k^2, \quad (4)$$

$$WBP_k = \left(\sum_{i=1}^M (I_{P_i}^2 + Q_{P_i}^2) \right)_k \quad (5)$$

where I_{P_i} and Q_{P_i} are the prompt correlation outputs at the tracking stage from the in-phase and quadrature arms, respectively. The values used in the experiments for M and K are 20 and 50, respectively.

3.2 Running DLL Variance

A non-coherent Early-Minus-Late (EML) discriminator is used in this particular experiment as the Delay

Lock Loop. According to [13], the EML discriminator can be written as:

$$DLL_i = \frac{\sqrt{I_{E_i}^2 + Q_{E_i}^2} - \sqrt{I_{L_i}^2 + Q_{L_i}^2}}{\sqrt{I_{E_i}^2 + Q_{E_i}^2} + \sqrt{I_{L_i}^2 + Q_{L_i}^2}} \quad (6)$$

where I_{E_i} and Q_{E_i} are the in-phase and quadrature correlation outputs of the early correlators, respectively (i.e., 0.25 chips early from the prompt correlation), I_{L_i} and Q_{L_i} are the in-phase and quadrature correlation outputs of the late correlators, respectively (i.e., 0.25 chips late from the prompt correlation). The DLL discriminator variance is then calculated from (6) for a running window of $N = 1000$ points.

3.3 Running PLL Variance

A two-quadrant ‘ATAN’ Costas discriminator is used in this experiment as a Phase Locked Loop. According to [13], the ATAN Costas discriminator can be written as:

$$PLL_i = ATAN\left(\frac{Q_{P_i}}{I_{P_i}}\right) \quad (7)$$

where I_{P_i} and Q_{P_i} are the prompt correlation outputs from the in-phase and quadrature arms, respectively. The Costas PLL discriminator variance is then computed from (7) for a running window of $N = 1000$ points.

3.4 Automatic Gain Control

Automatic Gain Control (AGC) is a key element in a GNSS receiver. The main responsibility of an AGC is to adjust the incoming signal power such that the quantization losses are kept as minimum as possible. Therefore, the AGC operation is usually directly coupled with the ADC. In case of a GNSS receiver, where the signal power remains below that of the thermal noise floor, the AGC is mostly driven by the ambient noise environment rather than the signal power. As a result, AGC can be utilized as an important tool for assessing the operating environment of any GNSS receiver.

Due to restrictions on emissions in and near the GNSS bands, it is quite likely that the AGC gain exclusively depends on the ambient noise environment rather than the GNSS signal power, as is expected in a typical interference-free situation. However, in case of an unlikely presence of interference, the AGC gain drops sharply in response to increased power in the GNSS band. This sharp immediate change in the AGC gain pattern can be utilized to indicate an intentional interference occurrence, as shown in Fig. 7. A metric, termed as AGC level changing rate, is used in this experiment for jamming detection. The AGC level changing rate can be calculated as follows:

$$\tau_i = \frac{x_i - x_{i-1}}{t_i - t_{i-1}}; i \geq 1 \quad (8)$$

where x_i is the measured AGC level at time t_i .

3.5 Running Digital Sum

The GNSS signal Interference Detection is performed via a Digital Sum (DS) check of the digitized signal after analog-to-digital conversion at the intermediate frequency. The DS is a function that sums the digital levels of the received digitized signal after ADC. The Digital Sum (DS) can be written as follows [11], [12]:

$$DS(k) = \frac{\sum_{i=1}^k a_i}{k} \quad (9)$$

where a_i is the digitized signal samples after ADC. For a 2-bit real quantization, a_i can take any values from the set $[\pm 1; \pm 3]$. Before calculating the digital sum, the bin distribution of a_i is converted from $[\pm 1; \pm 3]$ to $[\pm 1]$ as follows:

$$a_i = +1; a_i \geq 1, \quad (10)$$

$$a_i = -1; a_i \leq -1. \quad (11)$$

This is done in order to make sure that all digital levels have similar contributions to the final digital sum count. An example DS count is shown in Fig. 4 in a normal jamming-free scenario and a jamming scenario, where the DS counts are 1.3% in a normal jamming-free scenario and 10.8% in a jamming scenario with a maximum Jamming-to-Signal (J/S_{max}) ratio of 25 dB. The example DS counts are obtained with a front-end module from Sparkfun Electronics, named as SiGe GN3S sampler v3 [14]. The DS counts of the digitized signal levels after ADC in a nominal jamming-free environment should always be as close as possible to zero. In other words, the quantized bin distribution after ADC should be balanced such that there are

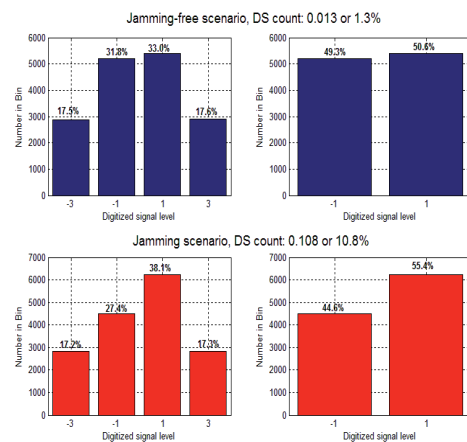


Fig. 4. Bin distribution of the digitized GNSS signal samples for 1 millisecond long data.

almost equal numbers of ‘+’ and ‘-’ levels in the digitized signal to avoid the presence of any DC bias in the signal. However, a small DC bias can always be present in a front-end module, but in any case it should always be fixed to a certain number. For example, the DC bias for the used SiGe GN3S sampler v3 front-end is less than 2%.

Finally, a Running DS (RDS) is calculated for smoothing the observations by the following equation:

$$RDS(j) = \frac{\sum_{k=j}^{j+N-1} |DS(k)|}{N}; \quad j = 1, 2, \dots \quad (12)$$

where a running window of $N = 1000$ is used in the experiment.

4. Experimental Setup

A software defined GNSS receiver platform, the FGI-GSRx, is used to process the raw IF data samples in post-mission. The FGI-GSRx has been developed for the analysis and validation of novel algorithms for an optimized GNSS navigation performance. The FGI-GSRx development was started from an open-source software radio platform introduced in [15]. In this particular experiment, besides the DLL and the PLL implementation, the C/N_0 estimation technique and the proposed RDS based interference detection method are implemented. A USB front-end module from Sparkfun Electronics, named as SiGe GN3S sampler v3 [14], is used to capture the raw GPS L1 C/A signal. The configuration of the SiGe radio front-end used in the experiment is mentioned in Tab. 1.

Intermediate Frequency	4.092 MHz
Front-end Bandwidth	2 MHz
Sampling Frequency	16.368 MHz
Number of Quantization bits	2 bits

Tab. 1. Front-end configuration for SiGe GN3S sampler v3.

Two different test scenarios are considered in the experiment: *i.* an intentional interference scenario with a maximum Jamming-to-Signal ratio (J/S_{max}) of 25 dB, and *ii.* an outdoor-indoor scenario without any intentional interference. The jamming-to-signal ratio, usually expressed in dB, is the ratio of the power of a jamming signal to that of a desired GNSS signal at a given point of a positioning receiver. The jammer signal was also constantly monitored with a spectrum analyzer during the test.

Many RF front ends today have implemented an integrated analog ADC and therefore it is almost impossible to read the settings and values from the AGC in the radio. Fortunately, for the purpose of calibrating the RF chain in a GNSS receiver, the RF often has a test pin for measuring the level of the AGC. This is intended to be used either with no RF input (or no signal) or with some predefined

calibration signal. The SiGe RF front end that is used in the GN3S sampler also has such a calibration pin [16]. The datasheet describes the above mentioned two test procedures, where the calibration signal level was set to -88 dBm. According to the datasheet, the test point should provide an output voltage of 1.2 V when no signal is present (maximum AGC gain) and 0.8 V when an L1 signal of -88 dBm is present at the RF input (minimum AGC gain). Unfortunately not much more information is available, but based on this and our measurements we have determined that when the noise level is increased the AGC voltage level is decreased.

5. Result Analysis

The impact of interference from the analyzed jammer on different GNSS receiver observables is shown in Figs. 4 to 7. The Covert GPS L1 jammer was turned on after about 56 seconds from the start of GNSS data capture with the SiGe front-end. The sudden drop in C/N_0 values for all the tracked satellites at the 56th second is clearly visible in Fig. 5. The approximate J/S_{max} is measured by monitoring the spectrum analyzer. This is also evident from Fig. 5 that the loss of C/N_0 due to jamming is at least 15 dB or more for all the tracked satellites.

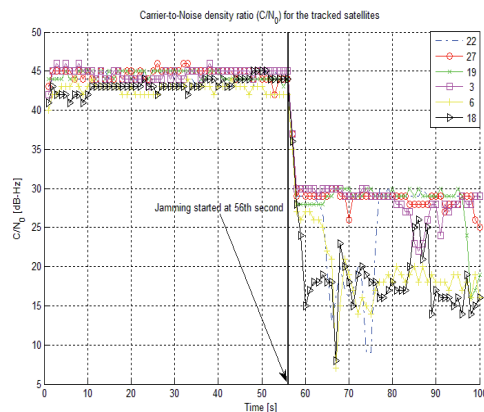


Fig. 5. C/N_0 for the tracked satellites in a jamming scenario with $J/S_{max} = 25$ dB.

The running DLL variance and the running PLL variance for one of the tracked satellites (i.e., PRN 27) in the presence of interference are shown in Figs. 6 and 7, respectively. The RDS of the digitized IF samples of the GNSS signal after ADC is also shown in Fig. 8. As shown in the figures, all these observables can successfully detect the interference occurrence almost immediately. The detection thresholds in all the above cases are computed against a false alarm probability of 0.01. However, it takes about 1 second for each of these techniques to stabilize due to the coarse code and frequency estimation at the acquisition stage, and therefore, they can only offer a detection decision after that time period. The output from the AGC block of the SiGe front-end is measured at 1 Hz rate via a PC-based PicoScope oscilloscope [17] connected through an USB port. The sudden drop of AGC levels during 56 to

59 second is evident from Fig. 9. Due to the presence of jamming signal on the GPS L1 band, the AGC block reacts almost immediately by lowering down the AGC gain values to a minimal level. The AGC level changing rate is shown Fig. 10. In a nominal environment where the temperature changes are steady, the only reason for such a huge drop in AGC is due to the presence of other unwanted RF signal in the GNSS spectrum. Therefore, the AGC level changing rate can be utilized to trigger any malicious interference occurrence by monitoring the AGC gain variations with respect to time.

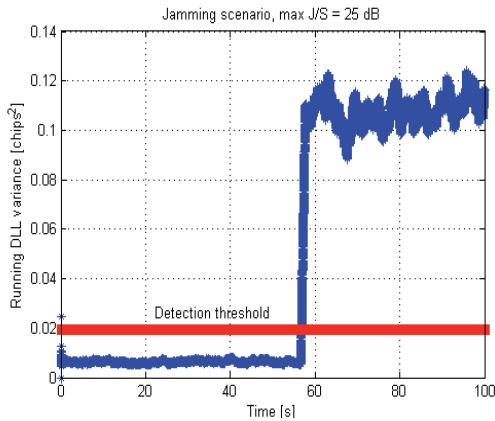


Fig. 6. Running DLL variance in a jamming scenario with $J/S_{max} = 25$ dB.

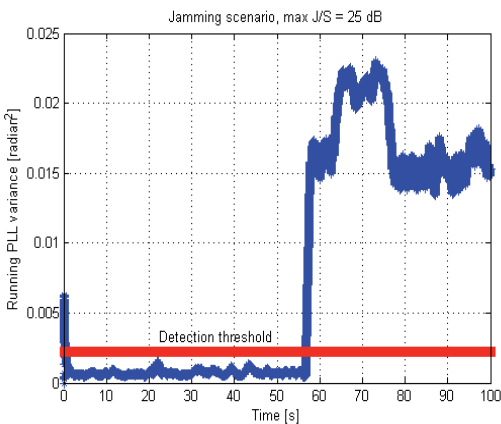


Fig. 7. Running PLL variance in a jamming scenario with $J/S_{max} = 25$ dB.

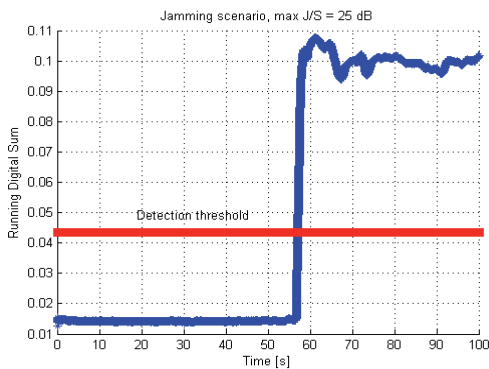


Fig. 8. RDS of the digitized IF samples in a jamming scenario with $J/S_{max} = 25$ dB.

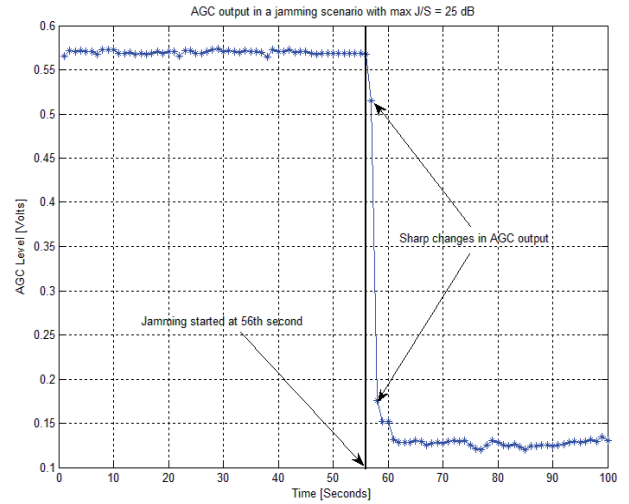


Fig. 9. AGC level in a jamming scenario with $J/S_{max} = 25$ dB.

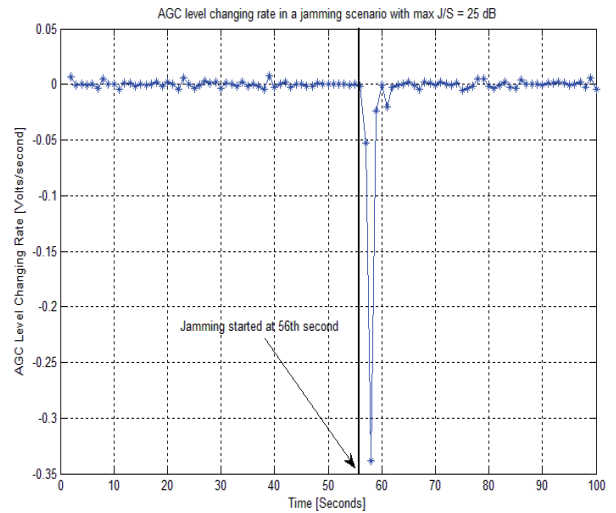


Fig. 10. AGC level changing rate in a jamming scenario with $J/S_{max} = 25$ dB.

The behavioral pattern of the analyzed receiver observables in a typical outdoor-indoor scenario are shown in Figs. 11 to 15. The tester was standing with the test equip-

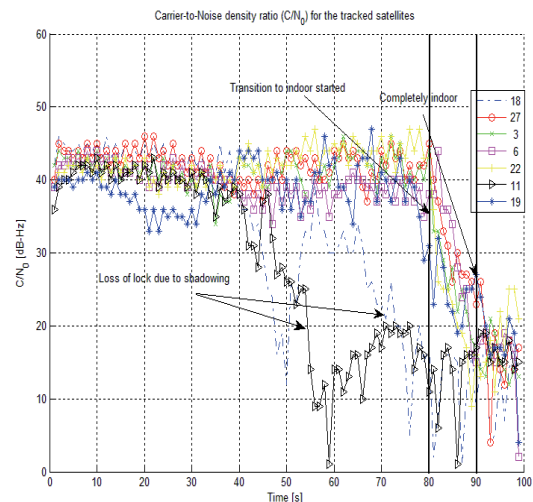


Fig. 11. C/N_0 for the tracked satellites in an outdoor-indoor scenario.

ment outside a typical three-story office building for about 40 seconds, after which he started walking into the office entrance for another 40 seconds. During the following 10 seconds (in between 80th and 90th seconds in the test), the tester was in the transition phase to walk from the outdoor to deep inside building made of concrete and steel, as can be seen from the sudden drop of C/N_0 in Fig. 11.

The running DLL variance and the running PLL variance of one of the tracked satellites (i.e., PRN 27) are shown in Figs. 12 and 13, respectively. It can be seen from these figures that both the variances increase due to the raise in the noise level, as the space-based GNSS signal faded away while moving towards indoor. The computed RDS of the digitized IF samples and the logged AGC level changing rate in this outdoor-indoor scenario are shown in Figs. 14 and 15, respectively. It can be seen from the figures that the computed RDS and the AGC gain is not at all affected by the increase in the noise level due to the signal fading while moving towards indoor.

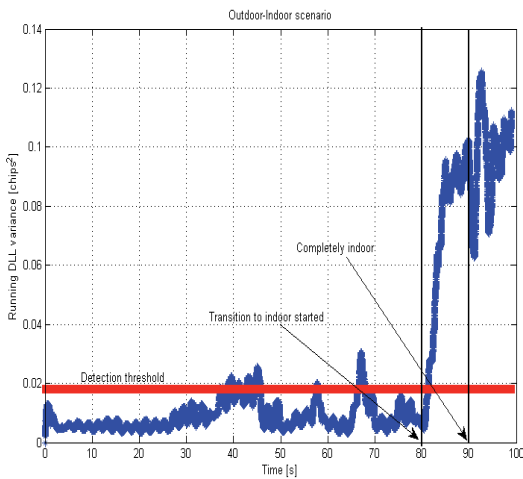


Fig. 12. Running DLL variance in an outdoor-indoor scenario.

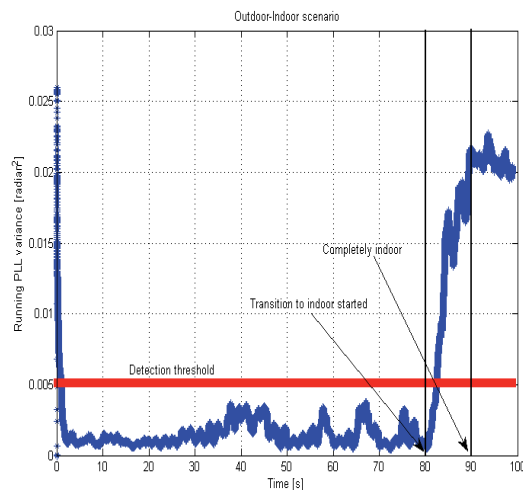


Fig. 13. Running PLL variance in an outdoor-indoor scenario.

The above results demonstrate the fact that the interference detection should only be based on such receiver observables which get affected only by the presence of interference, not by any other error source like shadowing

or weak signal condition. Hence, the most suitable receiver observables for interference detection are either the AGC output levels or the RDS count of the digitized signal levels. However, it is not always trivial to get access to AGC output, as it resides in the RF chain within the ADC block. Fortunately, the digitized signal levels are the output from the ADC block, which are then utilized by the acquisition and tracking blocks for further receiver-specific processing. While doing the receiver-specific processing, a simple RDS count on the digitized signal levels can be done to identify the presence of any malicious interference occurrence.

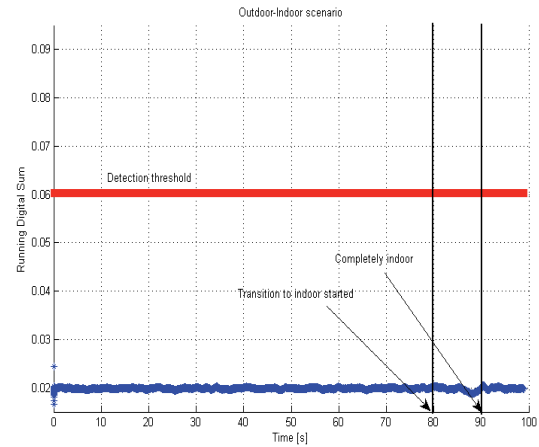


Fig. 14. RDS of the digitized IF samples in an outdoor-indoor scenario.

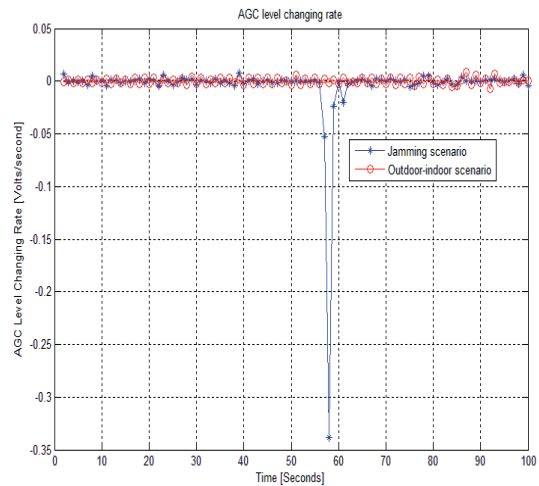


Fig. 15. AGC level changing rate in an outdoor-indoor scenario plotted on top of that of the jamming scenario presented in Fig. 10.

6. Conclusions

Five different receiver observables are investigated as candidate decision statistic for interference detection in two different environments: in the presence of intentional interference from an inexpensive car-jammer and in an outdoor-indoor environment without any intentional interference. The behavior of these observables in the above conditions

and their ability to uniquely identify an interference occurrence were addressed. It was shown that three of the receiver observables, i.e., C/N_0 , running DLL variance, and running PLL variance, cannot really distinguish the intentional interference occurrence from that of a weak signal condition as they react similarly in both the cases. It was also concluded that the proposed running digital sum of the digitized IF samples and the AGC output levels, can uniquely identify an intentional interference occurrence of a jammer as these observables do not get affected by the additive white Gaussian noise. The future work includes investigation of the proposed RDS based interference detection method in the presence of different interference sources (i.e., continuous wave interference, pulsed interference, etc.) with a variety of receiver front-ends from different manufacturers.

Acknowledgements

This research has been conducted within the project DETERJAM (Detection, analysis, and risk management of satellite navigation jamming) funded by the Scientific Advisory Board for Defense of the Finnish Ministry of Defense and the Finnish Geodetic Institute, Finland.

References

- [1] PULLEN, S., GAO, G. GNSS jamming in the name of privacy, potential threat to GPS aviation. *Inside GNSS*, USA, 2012, p. 34–43.
- [2] KRAUS, T., BAUERNFEIND, R., EISSFELLER, B. Survey of in-car jammers – analysis and modeling of the RF signals and IF samples (suitable for active signal cancellation). In *Proceedings of ION GNSS*. USA, 2011, p. 430–435.
- [3] MITCH, R.H., DOUGHERTY, R.C., PSIAKI, M.L., POWELL, S.P., O'HANLON, B.W., BHATTI, J.A., HUMPHREYS, T.E. Signal characteristics of civil GPS jammers. In *Proceedings of ION GNSS*. USA, 2011, p. 1907–1919.
- [4] KUUSNIEMI, H., AIROS, E., BHUIYAN, M.Z.H., KRÖGER, T. GNSS jammers: how vulnerable are consumer grade satellite navigation receivers? *European Journal of Navigation*, 2012, vol. 10, no. 2, p. 14–21.
- [5] PARKINSON, B.W., SPILKER, J.J. Jr. *Global Positioning System: Theory and Applications*. American Institute of Aeronautics, Vol. 1, 370 L'Enfant Promenade, SW, Washington, DC, USA, 1996, p. 390–392.
- [6] MOTELLA, B., SAVASTA, S., MARGARIA, D., DOVIS, F. A Method to assess robustness of GPS C/A code in presence of CW interferences. *International Journal of Navigation and Observation*, 2010, vol. 2010, Article ID 294525, 8 pages.
- [7] NDILI, A. Robust GPS autonomous signal quality monitoring. *PhD thesis*. USA, 1998, Department of Mechanical Engineering, Stanford University.
- [8] NDILI, A., ENGE, P. GPS receiver autonomous interference detection. In *Proceedings of IEEE PLANS*. USA, 1998.
- [9] BASTIDE, F., AKOS, D. M., MACABIAU, C., ROTURIER, B. Automatic Gain Control (AGC) as an interference assessment tool.

In *Proceedings of the 16th International Technical Meeting of the Satellite Division of the Institute of Navigation*. USA, 2003, p. 2042–2053.

- [10] ISOZ, O., BALAEI, A.T., AKOS, D.M. Interference detection and localization in the GPS L1 band. In *Proceedings of the International Technical Meeting of the Institute of Navigation*. USA, 2010, p. 925–929.
- [11] BISSELL, C., CHAPMAN, D. *Digital Signal Transmission*. Cambridge University Press, The Edinburgh building, Cambridge CB2 2RU, UK, 1992.
- [12] SMITH, D. R. *Digital Transmission Systems*. 3rd ed. Kluwer Academic Publishers, 3300 AH Dordrecht, The Netherlands, 2004, p. 260–261.
- [13] KAPLAN, E.D., HEGARTY, C. *Understanding GPS - Principles and Applications*. 2nd ed. Boston (USA): Artech House Publishers, 2006. Chapter 5.
- [14] SPARKFUN E. SiGe GN3S sampler v3. [Online] Cited 2013-10-29. Available at: <https://www.sparkfun.com/products/10981>.
- [15] BORRE, K., AKOS, D. M., BERTELSEN, N., RINDER, P., JENSEN, S.H. *A software-Defined GPS and Galileo Receiver: A Single-Frequency Approach*. 1st ed. Applied and Numerical Harmonic Analysis. Boston (USA): Birkhäuser Verlag GmbH, 2006.
- [16] SPARKFUN E. SiGe SE4120 Datasheet. [Online] Cited 2013-10-21. Available at: <http://media.digikey.com/pdf/Data%20Sheets/Skyworks%20PDFs/SE4120L.pdf>
- [17] PICOTECH PicoScope 4000 Series High-Resolution USB Oscilloscopes. [Online] Cited 2013-11-01. Available at: <http://www.picotech.com/picoscope4000.html>.

About Authors ...

Mohammad Zahidul H. BHUIYAN received his M.Sc. degree in 2006 and Ph.D. degree in 2011 from the Department of Communications Engineering, Tampere University of Technology, Finland. Dr. Bhuiyan is now working in the Department of Navigation and Positioning at the Finnish Geodetic Institute as a Specialist Research Scientist with research interests covering various aspects of GNSS receiver design and sensor fusion algorithms for seamless outdoor/indoor positioning.

Dr. Heidi KUUSNIEMI is a Research Manager at the Department of Navigation and Positioning at the Finnish Geodetic Institute, where she leads the research group on satellite and radio navigation. She is also a Lecturer at the Department of Surveying Sciences at Aalto University, Finland. She received her M.Sc. degree in 2002 and D.Sc. (Tech.) degree in 2005 from Tampere University of Technology, Finland. Her doctoral studies on personal satellite navigation were partly conducted at the Department of Geomatics Engineering at the University of Calgary, Canada. Her research interests cover various aspects of GNSS navigation, quality control, software defined receivers, multi-sensor fusion algorithms for seamless outdoor/indoor positioning, and GNSS interference mitigation methods. She is the President of the Nordic Institute of Navigation since 2011, and a member of the IEEE and the ION.

Mr. Stefan SÖDERHOLM is currently working as a Researcher at the Finnish Geodetic Institute, Department of Navigation and Positioning. He is working in many different areas focusing on improving the performance in consumer grade GNSS receivers. Before joining the Institute in September 2013 he was working at Fastrax Ltd since the end of 2000. The first 4 years at Fastrax he was developing GPS signal processing algorithms, navigation filters and GPS receiver integrity monitoring algorithms. From 2004 he headed the software development team and in 2008 he became Vice President of R&D in the company. In October 2012 Fastrax was acquired by u-Blox AG and before transferring to his current employer Stefan worked as a project manager and software developer in the Algorithm and Signal Processing team at uBlox. Stefan received his M.Sc. degree from Åbo Akademi University, Depart-

ment of Experimental Physics, in 1991 and his Licentiate degree from University of Turku, Dept. of Applied Physics, in 1996. Before joining Fastrax in 2000, Stefan was involved in various research projects in the fields of FT-IR and FT-Raman spectroscopy as well as molecular modeling and laser physics. In the field of GPS, Stefan has been the co-author of 9 conference papers and given numerous presentations on various topics. In other fields like FT-spectroscopy Stefan was the main author in two journal papers and numerous conference papers.

Mr. Esa AIROS received his M.Sc. degree in Electrical Engineering from the University of Lappeenranta. He is currently working as a research scientist at the Defense Forces Technical Research Centre. His research interests cover various electronic warfare applications including also GNSS.